

Orbital Period of the Dwarf Nova RXS J053234.9+624755 ¹

Ann B. Kapusta and John R. Thorstensen

*Department of Physics and Astronomy
6127 Wilder Laboratory, Dartmouth College
Hanover, NH 03755-3528;
ann.kapusta@dartmouth.edu*

ABSTRACT

We report spectroscopy of the newly discovered SU Ursae Majoris dwarf nova identified with the x-ray source RXS J053234.9+624755. Radial velocities of the H α emission line in the quiescent state give an orbital period of 0.05620(4) d (80.93 min), which is among the shortest for SU UMa stars with determined periods. We also report UBVI magnitudes of the quiescent dwarf nova and surrounding stars. Using a previous measurement of the superhump period, we find the fractional superhump excess ϵ to be 0.016(4), which is not atypical of dwarf novae in this period range.

Subject headings: stars – individual (RXS J053234.9+624755); binaries – close; dwarf novae, cataclysmic variables, SU UMa

1. Introduction

Cataclysmic Variables (CVs) are close binary systems that consist of an accreting white dwarf (the primary) and a secondary component that usually resembles a main-sequence star. Warner (1995) comprehensively reviews CVs. Dwarf novae, or U Geminorum stars, are a subclass of CVs that can be further subclassified based on their outburst behavior. The SU Ursae Majoris stars (referred to as UGSU) form a subclass of dwarf novae that undergo occasional superoutbursts in addition to normal outbursts. Superoutbursts occur less frequently than normal outbursts, but are brighter and last longer. During a superoutburst, characteristic oscillations called “superhumps” develop in the light curves. The measured superhump period, P_{sh} , is usually a few percent longer than the measured orbital period, P_{orb} . Almost all known SU UMa stars have $P_{\text{orb}} < 2$ hr. The superhump period excess, $\epsilon = [(P_{\text{sh}} - P_{\text{orb}})/P_{\text{orb}}]$, is an important quantity for these stars. Patterson (2001) demonstrated that ϵ correlates well with the mass ratio $q = M_2/M_1$, which is otherwise difficult to obtain.

¹Based on observations obtained at the MDM Observatory, operated by Dartmouth College, Columbia University, Ohio State University, and the University of Michigan.

Another class of dwarf novae are the WZ Sagittae stars (UGWZ), which are extreme examples of the SU UMa-type stars. WZ Sge stars exhibit large-amplitude outbursts (≥ 6 mag) that occur less frequently than the those of the UGSU (Osaki 1995). WZ Sge stars do exhibit superhumps in their light curves, but do not appear to have any ‘normal’ outbursts.

Here we present observations of the dwarf nova identified with the ROSAT x-ray source RXS J053234.9+624755 (hereafter RX0532+62). The discovery of this star, which lies in Camelopardalis, is described by Poyner & Shears (2006). Bernhard et al. (2005) classified it as a U Gem-type dwarf novae with a recurrence time scale of 133 days. The relatively frequent outbursts show that this star is not a UGWZ. RX0532+62 underwent a well-observed superoutburst in 2005 March. During this outburst a superhump period, P_{sh} , of 0.0571(2) d (82.2 mins) was reported by Tonny Vanmunster (CBA Belgium)²; Poyner & Shears (2006) independently found a similar, but less accurate, value of P_{sh} . We undertook observations of this star to independently determine the orbital period, P_{orb} , and allow determination of the superhump period excess, ϵ .

2. Observations

We took spectra using the MDM Observatory 1.3m McGraw-Hill telescope on Kitt Peak during two observing runs in 2005 September and 2006 January. We used the Mark III spectrograph and a thinned 1024² SITe CCD detector, with a 600 line mm⁻¹ grism that gave spectra spanning from 4500 Å to 7000 Å at 2.3 Å pixel⁻¹. In all, 106 spectra of RX0532+62 were taken with typical exposure times of 480 s, along with frequent comparison spectra to maintain the wavelength calibration. At the beginning and end of every photometric night, we observed flux standards to determine an absolute flux calibration. Table 1 gives a journal of observations. The system was in quiescence for all the observations reported here.

We also obtained direct images with the MDM 2.4m Hiltner Telescope. A SITe 2048² CCD with an image scale of 0.275 arcsec pixel⁻¹ was used, with filters matching the Johnson UBV and Kron-Cousins I passbands. The stars in the field were calibrated using Landolt (1992) standards. Exposures were obtained while the sky appeared photometric, and the reduced images were processed using the DAOPHOT program as implemented in IRAF³ (Stetson 1987). Positions for stars in the field were derived by fitting a plate model to 39 USNO A2.0 stars (Monet et al. 1996); the fit had an RMS error of 0.37 arcsec. Table 2 shows the celestial positions, magnitudes, and colors of RX0532+62 and the field stars. Figure 1 shows the field around RX0532+62 along with the measured V magnitudes.

²“Detection of Superhumps in the CV 1RXS J053234.9+624755” can be found at http://users.skynet.be/fa079980/cv_2005/1RXSJ053234_2005_mar_18.htm

³The Image Reduction and Analysis Facility software is written and maintained by the IRAF programming group located at the National Optical Astronomy Observatory (NOAO). Software and information can be found at <http://iraf.noao.edu>.

We reduced the spectra using standard IRAF routines, except for the extraction of one-dimensional spectra from the two-dimensional images. For this, we used an original implementation of the optimal extraction algorithm developed by Horne (1986); the primary advantage over the IRAF *apsum* routine was an improved rejection of bad pixels. The time averaged and flux-calibrated spectrum of RX0532+62 is shown in Figure 2. The spectrum appears typical of dwarf novae, showing strong broad emission lines. The double peaks in the emission lines imply that the orbital inclination is not too far from edge-on. To measure the emission line radial velocities we used the convolution method described by Schneider & Young (1980). The steep sides of the line profile were measured by convolving the line with a function consisting of positive and negative gaussians displaced by an adjustable separation. The emission lines’ widths and strengths were measured in the time-average spectra; the results are given in Table 3.

To search for P_{orb} in the radial velocities, we used the “residualgram” method as described by Thorstensen et al. (1996). Figure 3 shows the result for the 2005 September data. Table 4 gives the parameters of the best sine fits of the form $v(t) = \gamma + K \sin[2\pi(t - T_o)/P]$, and the rms scatter σ around the best fits. Figure 4 shows the velocities folded on the period adopted from the combined (2005 September, 2006 January) data, together with the best-fitting sinusoid. The 2005 September data did not unambiguously determine the correct choice of daily cycle count because of the limited hour angle coverage available early in the observing season. The 2006 January data were taken in order to resolve the ambiguity, but for unknown reasons the velocities had greater scatter than the 2005 September data. We also measured velocities of the $H\beta$ emission in an attempt to resolve the daily cycle count. The $H\beta$ velocities corroborated the $H\alpha$ measurements, but the period remained ambiguous. However, we know P_{sh} , and that the P_{orb} of an SU UMa-type should be a few percent less than P_{sh} . This guides our choice of cycle count, which yields 0.05620(4) d for the 2005 September data. The run-to-run cycle count is ambiguous, but periods consistent with all the data are given by

$$P_{\text{orb}} = \frac{130.588 \pm 0.015}{2324 \pm 6} \text{ d},$$

where the numerator is the measured interval between blue-to-red crossings of the $H\alpha$ emission velocities determined from our two observing runs, and the denominator is constrained to integer values.

3. Discussion

Combining our P_{orb} with the previously measured P_{sh} , we find $\epsilon = 0.016(4)$. Patterson et al. (2003) plot $\log(\epsilon)$ against $\log(P_{\text{orb}})$ for a large number of systems with hydrogen-rich secondaries. On this plot, RX0532+62 lies near the short-period end, where systems appear to be evolving through the period minimum. These occupy a relatively wide range of ϵ values. RX0532+62 is toward the top of this range, as if it has evolved into the turnaround region relatively recently. Patterson (2001) fits the empirical relation between ϵ and the mass ratio q as $\epsilon(q) = 0.216q$. Using

our ϵ value, we determine $q = 0.074(19)$, which is typical for dwarf novae with similar periods⁴. We conclude that RX0532+62 is a typical SU UMa star lying near the minimum period for hydrogen-rich secondary systems.

Acknowledgments: We thank Holly Sheets for taking the 2006 January spectra. The National Science Foundation funded this research through award AST-0307413 and an REU supplement to that award. Travel for Ann Kapusta was made possible by a generous gift from Claudia and Jay Weed.

⁴The uncertainty in q is computed here using only the uncertainty in ϵ ; imperfections in the empirical relation are ignored.

REFERENCES

- Bernhard, K., Lloyd, C., berthold, T., Kriebel, W., Renz, W. 2005, IBVS, 5620
- Horne, K. 1986, PASP, 98, 609
- Landolt, A. U. 1992, AJ, 104, 340
- Monet, D., et al. 1996, USNO-SA2.0, (U. S. Naval Observatory, Washington, DC)
- Patterson, J. 2001, PASP, 113, 736-747
- Patterson, J., et al. 2003, PASP, 115, 1308-1329
- Poyner, G. & Shears J. 2006, J.Br. Astron. Association, 116, 1
- Osaki, Yoji 1995, PASJ, 47, 47-58
- Thorstensen, J. R., Patterson, J., Thomas, G., & Shambrook, A. 1996, PASP, 108, 73
- Stetson, P. B., 1987, PASP, 99, 191
- Schneider, D., & Young, P. 1980, ApJ, 238, 946
- Warner, B. 1995, Cataclysmic Variables (Cambridge University Press)

Table 1. Journal of Observations

Dates(UT)	N^a	HA Start ^b	HA End ^c
Spectroscopy (1.3m)			
2005 Sep 13	23	−5 : 01	−1 : 32
2005 Sep 14	17	−4 : 10	−1 : 41
2005 Sep 15	13	−3 : 01	−1 : 15
2005 Sep 16	18	−5 : 07	−2 : 38
2006 Jan 22	10	+2 : 16	+4 : 10
2006 Jan 23	25	−2 : 55	+0 : 33
UBVI Direct Imaging (2.4m)			
2005 Sep 14	4	−1:03	−0:59

^aNumber of Exposures

^bHour angle at the midpoint of the first exposure in hours and minutes

^cHour angle at the midpoint of the exposure in hours and minutes

Table 2. Filter Photometry

α^a	δ^a	$U - B$	$B - V$	V	$V - I$
Field stars					
5:32:15.52	+62:46:28.3	1.24 ± 0.02	1.19 ± 0.01	13.87 ± 0.00	1.21 ± 0.01
5:32:15.99	+62:47:23.7	0.24 ± 0.03	0.73 ± 0.01	15.94 ± 0.01	0.84 ± 0.01
5:32:17.30	+62:47:17.9	0.62 ± 0.14	0.91 ± 0.02	16.98 ± 0.01	1.04 ± 0.01
5:32:23.84	+62:49:30.5	0.38 ± 0.11	0.88 ± 0.03	17.00 ± 0.02	0.94 ± 0.03
5:32:26.39	+62:48:49.9	0.84 ± 0.06	1.09 ± 0.01	15.59 ± 0.01	1.18 ± 0.01
5:32:29.45	+62:46:02.9	0.21 ± 0.02	0.68 ± 0.01	14.97 ± 0.00	0.78 ± 0.01
5:32:30.82	+62:49:49.3	0.45 ± 0.01	0.85 ± 0.01	14.21 ± 0.00	0.86 ± 0.00
5:32:30.96	+62:50:06.6	0.17 ± 0.26	0.92 ± 0.06	17.86 ± 0.02	1.04 ± 0.03
5:32:31.46	+62:47:58.1	0.20 ± 0.03	0.75 ± 0.01	15.62 ± 0.01	0.84 ± 0.01
5:32:32.18	+62:49:39.0	1.42 ± 0.04	1.29 ± 0.01	14.40 ± 0.00	1.29 ± 0.00
5:32:37.91	+62:49:54.1	0.27 ± 0.05	0.78 ± 0.01	16.12 ± 0.01	0.85 ± 0.01
5:32:39.68	+62:46:29.3	0.40 ± 0.01	0.84 ± 0.00	14.31 ± 0.00	0.94 ± 0.01
5:32:39.69	+62:50:10.7	0.44 ± 0.19	0.87 ± 0.03	17.45 ± 0.01	0.98 ± 0.02
5:32:40.04	+62:47:45.1	0.89 ± 0.38	1.30 ± 0.04	17.32 ± 0.01	1.34 ± 0.02
5:32:40.46	+62:46:23.5	0.96 ± 0.17	0.99 ± 0.03	16.91 ± 0.01	1.06 ± 0.01
5:32:44.65	+62:45:39.9	0.39 ± 0.01	0.84 ± 0.01	14.13 ± 0.01	0.87 ± 0.01
5:32:46.49	+62:45:48.1	0.17 ± 0.04	0.80 ± 0.01	15.84 ± 0.01	0.84 ± 0.01
5:32:47.28	+62:47:55.8	0.67 ± 0.24	0.91 ± 0.04	17.45 ± 0.01	0.97 ± 0.02
5:32:48.62	+62:47:20.6	1.46 ± 0.65	1.13 ± 0.05	17.74 ± 0.02	1.21 ± 0.02
5:32:49.35	+62:47:35.3	0.15 ± 0.16	0.81 ± 0.04	17.64 ± 0.01	0.95 ± 0.02
5:32:49.44	+62:48:22.9	0.21 ± 0.04	0.74 ± 0.01	16.05 ± 0.01	0.80 ± 0.01
5:32:49.82	+62:48:12.4	1.12 ± 0.18	1.16 ± 0.02	16.45 ± 0.01	1.22 ± 0.01
5:32:50.98	+62:46:16.5	0.10 ± 0.01	0.61 ± 0.01	13.47 ± 0.01	0.63 ± 0.01
5:32:52.02	+62:46:18.8	0.19 ± 0.13	0.88 ± 0.02	16.70 ± 0.01	0.94 ± 0.01
5:32:52.04	+62:49:10.8	0.46 ± 0.10	0.97 ± 0.02	16.78 ± 0.01	1.02 ± 0.02
5:32:54.02	+62:48:58.2	1.28 ± 0.55	1.26 ± 0.06	17.78 ± 0.02	1.42 ± 0.02
Variable star					
5:32:33.88	+62:47:52.5	-1.19 ± 0.01	0.01 ± 0.01	16.25 ± 0.01	0.65 ± 0.01

^aCoordinates referred to the ICRS(i.e. J2000), and are from a fit to 39 USNO A2.0 stars, with a scatter of 0.37 arcsec. Right ascensions are measured in hours, minutes,

and seconds and the declinations are in degrees, minutes, and seconds.

Table 3. Emission Features

Feature	E.W. ^a (Å)	Flux ^b	FWHM ^c (Å)
RX 0532+62			
H β	113	1844	32
HeI λ 4921	10	162	40
HeI λ 5015	12	184	37
Fe λ 5169	9	139	36
HeI λ 5876	43	524	40
H α	160	2004	35
HeI λ 6678	20	236	46

^aEmission equivalent widths are counted as positive.

^bAbsolute line fluxes in units of 10^{-16} erg cm $^{-2}$ s $^{-1}$. These are uncertain by a factor of about 2, but relative fluxes of strong lines are estimated accurate to ~ 10 per cent.

^cFrom Gaussian fits.

Table 4. Fit to the Radial Velocities

Data Set	T_0^{a}	P (days)	K (km s ⁻¹)	γ (km s ⁻¹)	N	σ^{b} (km s ⁻¹)
Combined	53629.9522(15)	[0.0561950] ^c	38(6)	−0(5)	106	23
2005 September	53627.9854(10)	0.05620(4)	42(4)	7(3)	71	19
2006 January	53758.580(2)	0.0557(3)	38(10)	−9(7)	35	23

Note. — Parameters of least-squares sinusoid fits to the radial velocities, of the form $v(t) = \gamma + K \sin(2\pi(t - T_0)/P)$.

^aHJD - 2452000.

^bRoot-mean-square residual of the fit.

^cThis period is based on an arbitrary choice of cycle count between 2005 September and 2006 January.

Fig. 1.— Finding chart with standard magnitudes. The image is approximately 4.5 arc minutes square. The labels are V-Magnitudes of stars in the field.

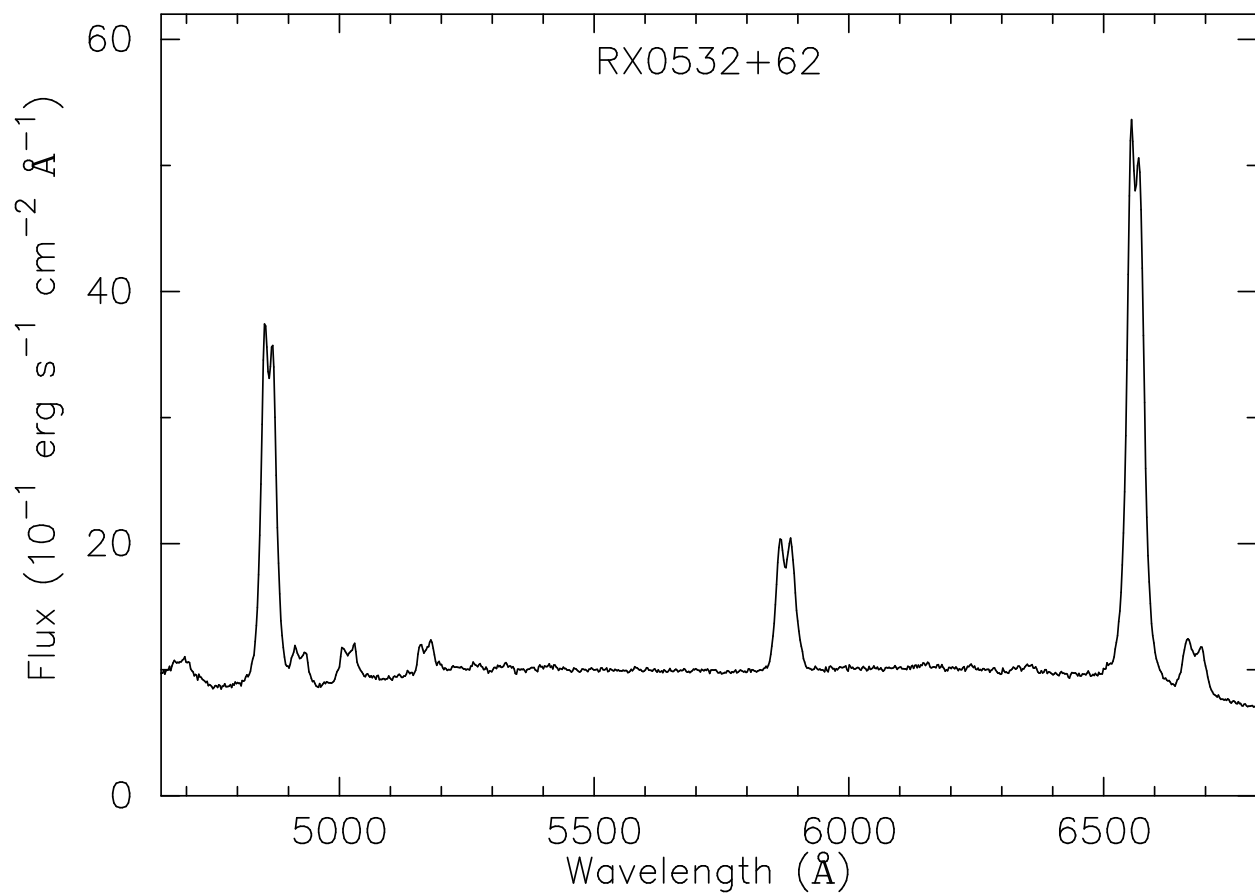


Fig. 2.— Mean spectrum of RX0532+62 from 2005 September. The 2006 January average appeared nearly identical.

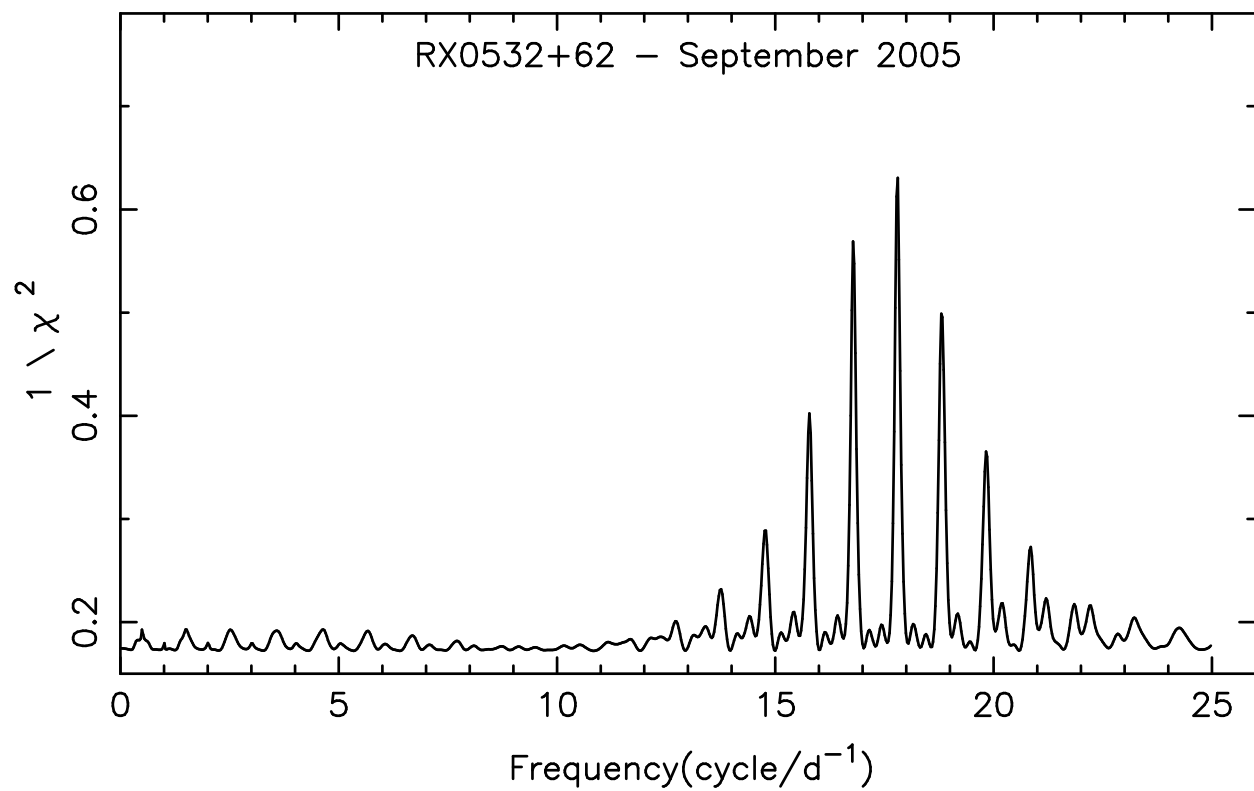


Fig. 3.— Results of the period search on the H α radial velocities of RX0532+62. The highest peak corresponds to the adopted P_{orb} .

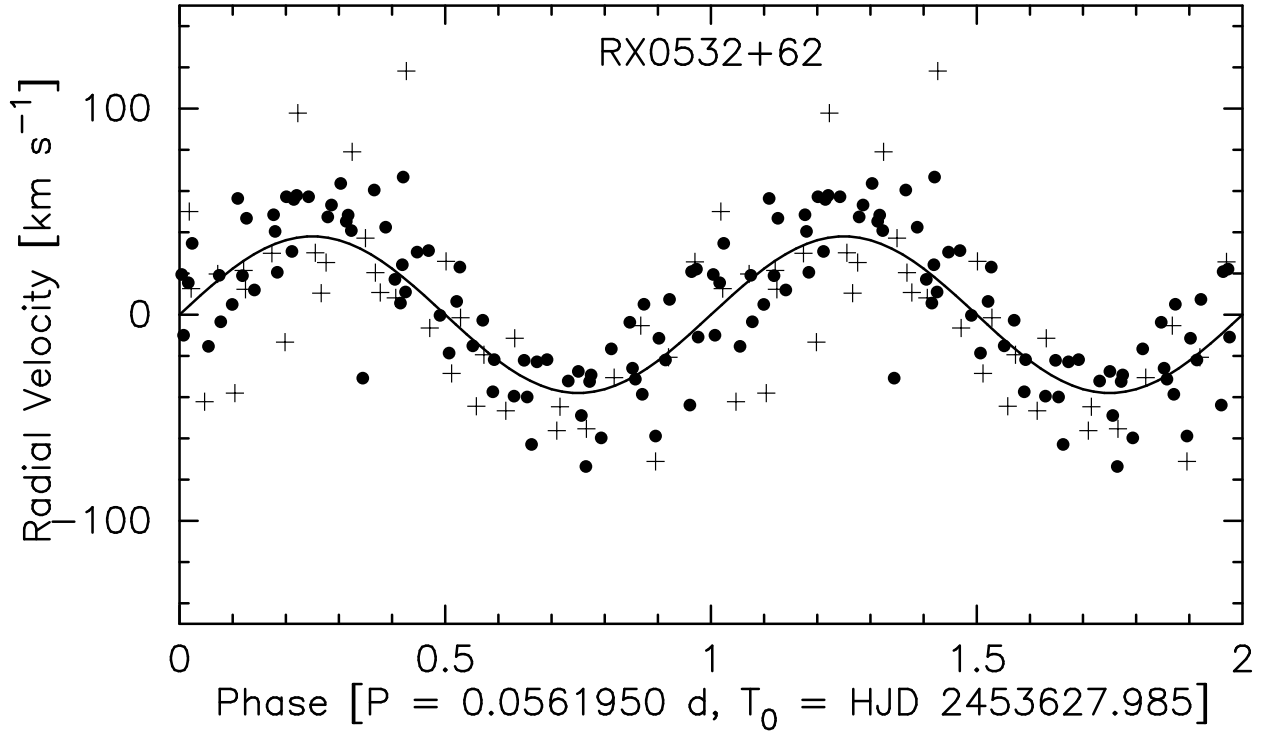


Fig. 4.— Emission-line radial velocities as a function of orbital phase, together with the best-fitting sinusoid. The data and fit are repeated for a second cycle to preserve continuity. The pluses show velocities from 2006 January, and the filled circles are from 2005 September. The gross period is determined by the 2005 September data and comparison to the superhump period, but the precise period used here is based on an arbitrary choice of cycle count between the 2005 September and the 2006 January observing runs.

This figure "figure1.png" is available in "png" format from:

<http://arxiv.org/ps/astro-ph/0607071v1>